Current Trends in Biotechnology and Pharmacy
Vol. 18(2) 1688-1696, April 2024, ISSN 0973-8916 (Print), 2230-7303 (Online)
DOI: 10.5530/ctbp.2024.2.17

Targeting Glucose Metabolism in Diabetes-A Homology Modeling and Active Site Identification for Inositol Monophosphatase

Lavanya Gnanam[1] and Navaneetha Nambigari[1, 2*]

[1]Department of Chemistry, University College of Science, Saifabad, Osmania University, Hyderabad - 500004, Telangana State, India.
[2]Department of Chemistry, University College of Science, Osmania University, Hyderabad - 500007, Telangana State, India.
[*]Corresponding author: navaneeta@osmania.ac.in

Abstract

Diabetes is a degenerative disease caused by either the body's inability to use insulin adequately or the pancreas's failure to release enough insulin. Diabetes is a glucose metabolic imbalance produced by the phosphodiesterase family of protein inositol monophosphatase (IMPase). Inositol monophosphatase, an enzyme involved in the phosphatidylinositol signalling pathway, is encoded by the IMPA1 gene.

Homology Modelling is used to create a 3D model of the IMPA1 protein (target). The FASTA sequence for the IMPase protein (265 amino acids) (Uniprot ID H0YBL1) is obtained from the Uniprot server. Jpred, and NCBI Blast servers are used to search for templates. Based on the query coverage (92%) and E-score, the protein with the PDB ID-1IMA is identified as a potential template. The structural alignment (by ClustalW) submitted to the SWISS-MODEL service yields a 3D model. The Swiss PDB viewer is used to minimise energy (E = - 10099.60 kcal/mole). Procheck, ERRAT, and the VERIFY 3D server validate the model.

The Ramachandran plot of the 3D model indicates that 93.5% of the amino acids are in the allowed region and none are in the forbidden region. The ERRAT result shows an overall quality factor of up to 96.17% for non-bonded atomic interactions. According to NCBI blast, the conserved domain is between 60 - 245 amino acids. The servers (ACTIVE SITE FINDER,) indicate binding pockets in the hydrophobic area, and Swiss dock is used to determine the active residues by protein - small ligand (Natural substrate, Fructose Biphosphatase- FBPase receptor) docking to identify the active site residues (Asp 90 and Thr- 95) based on visualisations and a Swiss energy value. The glucose metabolism can be stopped by blocking these residues. Key Words: Diabetes, Phosphodiesterase family, Homology Modelling

Introduction

Diabetes is the world's most serious health concern and the second biggest cause of mortality. Diabetes affects 537 million persons aged 20 to 79. Diabetes is expected to affect 643 million people by 2030 and 783 million by 2045. Three out of every four diabetic adults reside in low- and middle-income nations. Prevalence has been growing faster in low- and middle-income nations than in high-income countries. Diabetes and renal disease caused an estimated 2 million deaths in 2019 (1). In contrast, the likelihood of dying from any of the four major non-communicable illnesses (cardiovascular diseases, cancer, chronic respi-

ratory diseases, or diabetes) between the ages of 30 and 70 reduced by 22% globally.

Inositol monophosphatase 1 (IMPase) was shown to be significantly expressed in Triple Negative Breast Cancer (TNBC) tissues and to play carcinogenic functions via the mTOR pathway and the EMT process, making it an appealing method for boosting the treatment response of IMPA1-high TNBC tumours (3).

IMPase is necessary for dephosphorylating inositol monophosphates to produce inositol (4), which is a key metabolite as a precursor for producing phosphoinositide and hence has dramatic effects on gene expression and is essential for cell signalling and biological activities (5). Recent research has linked disruption of the inositol cycle to a number of human illnesses, including cancer, neurological disorders, and diabetes (6).

The Akt-mediated pathway is known to be involved in cell survival, growth, proliferation, angiogenesis, and glucose metabolism activation. It has been proven to be closely related to pulmonary hypertension(PAH) aetiology (7, 8). The proper synthesis or recycling of myo-inositol, the key precursor of all phosphatidylinositols, including phosphatidylinositol 3,4,5-trisphosphate (PIP3), which binds to Akt and recruits it to the plasma membrane, is required for this pathway to be activated. since a result, the molecular processes involved in myoinositol production or recycling are critical, since they may influence the shift into a highly proliferative phenotype.

Inositol monophosphatase 1 (IMPase) is a cytosolic enzyme that converts the highly osmotic glucose metabolite glucose 6-phosphate (G6P) to nonosmotic myo-inositol, therefore protecting cells from osmotic stress (9). Based on this feature, IMPA1 has been identified as a major contributor to the inositol cycle, including both de novo inositol synthesis and inositol polyphosphate recycling (10, 11). One of the most prominent features of PAH is metabolic reprogramming of the pulmonary vascular cells, which results in an increase in glucose absorption and metabolism.

Materials and Methods

The Homology modelling approach predicts the 3D structure of a protein as precisely as a low-resolution experimentally validated structure (12). The structural model of the target is created using sequence alignment and template structure (13). The protein's 3D structure is essential to understand its biology; comparative modelling approach. The amino acid sequence of the target protein (Uniprot ID: H0YBL1 _ HUMAN) is downloaded in FASTA format from the ExPASy Swiss-Prot (Expert protein analysis system) site (http://www.expasy.org).(14). Position -specific Iterative Basic Local Alignment Search Tool (PSI -BLAST) (15) Jpred (16) are used for template search. It is one of the most often used methodologies for protein structure prediction.

The pairwise alignment of the target protein, with the sequence of selected template is carried out with Clustal W tool which is a series of widely used computer programs used in Bioinformatics for multiple sequence alignment (17). The alignment file is used for model generation using the Swiss model (18). The protein structures are visualized and analyzed with SPDBV, which is an interactive molecular graphics program which analyzes several proteins at the same time (19). Clustal W is used to perform pairwise alignment of the target protein with the sequence of the selected template (17). The alignment file is used to generate models using the Swiss model (18). SPDBV, an interactive molecular graphics programme that analyses many proteins at the same time, is used to visualize and analyze the protein structures (19).

The refinement of the target protein's initial model is followed by energy minimization. SPDBV is used to minimize energy using a preset cutoff Root Mean Square Deviation (RMSD) of 0.3 A°. PROCHECK from the Structural Analysis and Verification Server (SAVES) validates

the model (20) predict the stereochemical quality of the resulting protein 3D model (21, 22). By measuring the dihedral angles phi and psi of the amino acid residues, the angle at the peptide bond is typically 180° because the partial double-bond feature preserves the peptide planar (23). ProSA server evaluates the quality of the local model (24).

Active Site Prediction

Prediction of ligand-binding sites, a critical step in understanding a protein's molecular recognition mechanism and function. The putative active site was determined using the portion of the IMPase protein that binds to its receptor. The binding domain facilitates the interaction of IMPase with FBPase receptor proteins, resulting in the activation of a conserved pathway that governs critical elements of cell fate determination, migration, and polarity. The Active Site Finder server identifies the protein's active site area. The Protein Active Site Prediction service computes the cavities in a particular protein. The prediction of ligand-binding sites is a critical step in understanding a protein's molecular recognition mechanism and function (25). The identification of putative binding residues, active site prediction servers such as CASTp (26). The specific binding residues within the binding domain of the target protein.

Results and Discussion

Using homology modelling, a 3D model of the IMPase protein was created. The IMPase protein amino acid sequence (UniprotKB ID: H0YBL1) was sent to template search server programmes such as NCBI BLAST and JPred to locate a suitable template sequence, and the results are shown in Table 1. Based on factors like as identity, sequence similarity, and E - value, the protein with the PDB ID - 1IMA is chosen as a template. 1IMA template protein shows a query coverage of is 92% and a sequence identity of 87.7% with the IMPase protein. As a consequence, the 1IMA protein is used as a template for creating the 3D model of the IMPase protein. ClustalW was used to perform pair-wise sequence alignment between the IMPase protein and the template protein 1IMA, as shown in Figure 1. The SWISS MODEL was used to construct the homology model once the alignment file and template coordinates were given.

Table 1: Tools for template Search.

S.No.	Server	E- Score	Template (PDB)
1.	NCBI	4e-178	1IMA
2.	JPred	1e-135	1IMA

Figure 1. Alignment of Target (HoYBL1) and template sequence using Clustal W.

The 3D model (*Figure 2*) was considered for further refinement and validation studies. Similar techniques were reported earlier for the identification of template and model building (27 - 29).

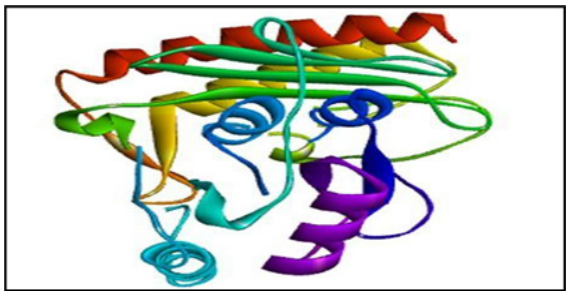

Figure 2: 3D model of IMPase protein.

The 3D model is further energy minimized using Swiss- PDB viewer (19) to assess the reliability of the generated 3D structure. The energies before and after energy minimization were –9476.8 kJ/mol and –10099.6 kJ/ mol respectively. The stereochemical quality of the protein structure was assessed by using Ramachandran plot (21) (*Figure 3*), which shows 202 (93.5%) of residues in the energetically most favored region, 13 (6%) of residues in the additionally allowed region, 1(0.5%) of the residues in the generously allowed region and none (0%) in the disallowed region. It can be seen that most of the amino acid residues are in the energetically favored region (Table 2). This shows that the protein was stereo chemically good which was generated after energy minimization.

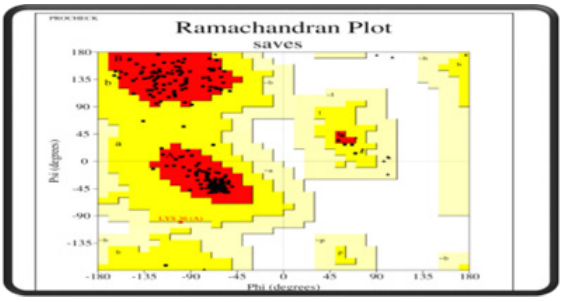

Figure 3. Ramachandran plot of the 3D protein.

Ramachandran plot obtained by Structural Analysis and Verification Server (SAVES). The red color in the plot indicates the most favorable region, yellow represents additionally allowed, light yellow indicates generously allowed and white field indicates disallowed region.

Table 2. Ramachandran plot statistics

RESIDUES IN THE FOLLOWING REGION	NO.OF RESIDUES	PERCENTAGE
MOST FAVORED REGION[A,B,L]	202	93.5%
ADDITIONAL ALLOWED REGION [a, b, l, p]	13	6.0%
GENEROUSLY ALLOWED REGION[-a, -b, -l, -p]	1	0.5%
DISALLOWED REGION	0	0.0%
NO. OF NON- GLYCINE AND PROLINE RESIDUES	216	
NO. OF END RESIDUES (GLYCINE, PROLINE)	14	
NO. OF GLYCINE RESIDUES (SHOWN AS TRIANGLES)	20	
NO. OF PROLINE RESIDUES	8	
TOTAL NUMBER OF RESIDUES : 258		

The Figure 4 depicts the Verify3D compatibility of the IMPase protein model (3D) with its own amino acid sequence (1D) (30, 31). The Verify3D server ascertained whether an atomic 1IMA model (3D) was compatible with its amino acid sequence (1D). For each of the 265 residues, the scores of a sliding 21-residue window (from –10 to +10) are added and plotted. The average 3D-1D score of 84.50 % of the residues is greater than 0.2.

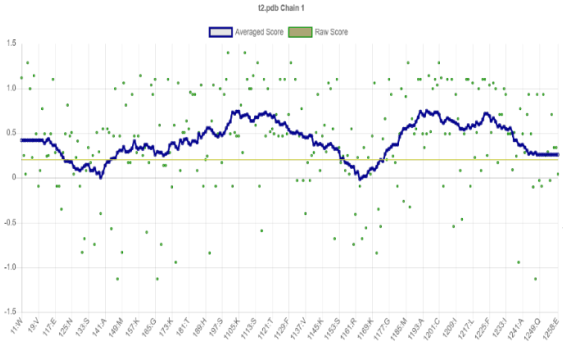

Figure 4. VERIFY 3D plot.

The validation of the selected protein after energy minimization is by PROCHECK and ProSA .The ProSA plot gives the local model quality (Figure 5) of the IMPase protein. The low

Z-score indicates a high overall model quality and compares the deviation of the ProSA server to calculate the energy required for protein folding architecture as a function of the amino acid sequence.

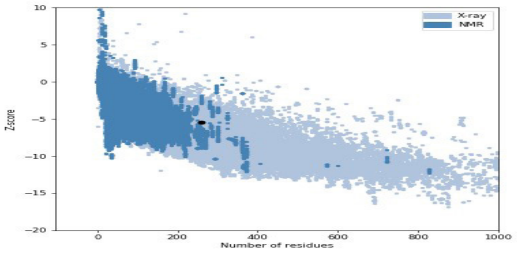

Figure 5. ProSA plot of IMPase. Black spot represents the 3D model falls in the NMR region with the Z- score= -5.42.

ProSA-Web Z-score determined by X-ray crystallography (light blue) and NMR spectroscopy for all proteins in the PDB (dark blue). The black spot in Figure 5 corresponds to the IMPase protein and has the Z-score value of –5.42.The low Z-score indicates good overall model quality and compares the structure's total energy deviation from an energy distribution derived from native conformations.

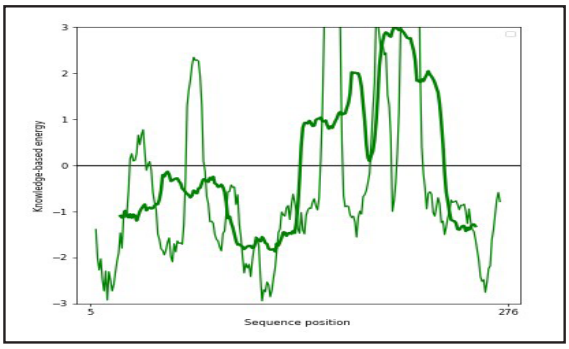

Figure 6. ProSA plot Energy Profile.

Overall, the folding energies of the protein residues are quite negative, with the model protein's folding energy in the range of native conformations having a Z-score of -5. 42. Figure 6 depicts the charting of energy as a function of amino acid sequence position. Positive values, in general, refer to problematic or incorrect sections of the input structure. The validation server tool findings indicate that the produced 3D structure of IMPase protein is stereo chemically and energetically stable. As a result, this protein is trustworthy for future research.

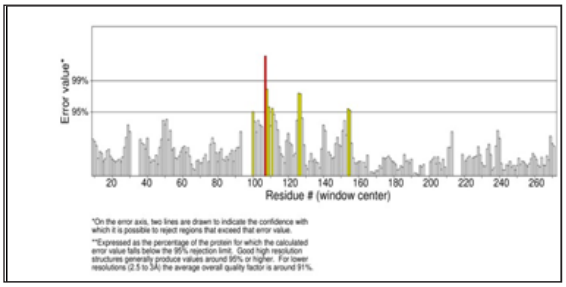

Figure 7. ERRAT Profile.

ERRAT is a program for verifying protein structures determined by crystallography. Error values are plotted as a function of the position of a sliding 9-residue window. The ERRAT Profile of the IMPase 3D model shows an overall quality factor of 96.17, against an average qulity factor 91% for a resolution of 2.5 – 3.0Å (32). The result of the ERRAT server shows a graph between residues and error values (Figure.7). The overall quality score of this input structure is 96.17% and this is considered good. If the input structure has good resolution, then it should have a quality score of greater than 95%.

IMPase has three hydrophilic hollow active sites, each of which bind water and magnesium molecules. The 3D Structure of the IMPase protein generated by homology modeling is presented in Figure 3. The detailed secondary structure of the protein is shown in Figure 8. The structure constitutes 9 Helices, 17 loops, 14 β sheets.

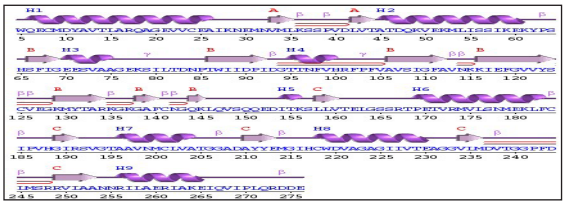

Figure 8. Secondary Structure of IMPase protein.

Current Trends in Biotechnology and Pharmacy
Vol. 18(2) 1688-1696, April 2024, ISSN 0973-8916 (Print), 2230-7303 (Online)
DOI: 10.5530/ctbp.2024.2.17

The secondary structure details along with the amino acid chain lengths are shown in Table 3. The topology of the target protein is shown in Figure 9. The topological analysis reveals that the N terminal region (Trp 5) and C terminal terminal region (Ile 266).

Table 3. Secondary structure Of IMPase protein

HELICES	LOOPS	BETA SHEETS
Q 6 - A 26	5W	V 33 – L 35
A 45 – K 61	Y 62 – H 64	L42 – T 44
E 70 – A 75	G 76 – P 85	S 66 – G 69
T 95 – H 100	V 113 – K 115	T 86 – I 92
I 154 – K 156	C 125 – G 128	A 106 – A 112
P 169- F 183	K 135 – K 137	K 116 – S 124
A 196 – A 204	C 141 – G 143	K 129 – R 134
C 218 – E 230	L 146 – D 153	G 138 – F 140
R 256 – E 265	S 153	Q 144 – K 145
	T 161 – T 168	L 158- V 160
	C 184 – H 188	G 188- R 191
	S 192 – T 195	A 210 – E 213
	T 205 – D 209	V 234 – M 236
	M 214- H 217	R 249 A 253
	A 231 – G 233	
	D 237 – R 248	
	N 254 – N255	

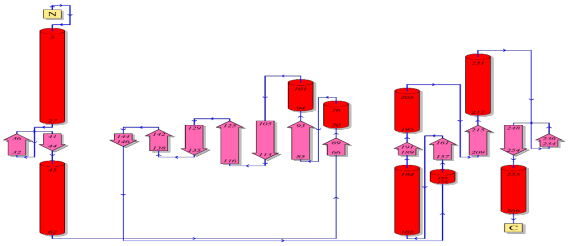

Figure 9. Topology of the amino acid residues

The conserved domains of the IMPase protein are characterized using the NCBI BLAST tool, as illustrated in Figure 10; NCBI blast also identified the binding site domains of the IMPase protein. The results demonstrate that the target protein includes a FIG domain (Amino Acid 28 – 264) from Insilico predictions of protein interactions utilising protein-ligand docking studies enable the discovery of major residue-residue contacts involving target interactions. IMPase protein binding site residues and cavity volumes were predicted using Active Site Finder based on hydrophobicity. SWISS dock server was used to perform protein-natural ligand docking between IMPase and FBPase proteins.

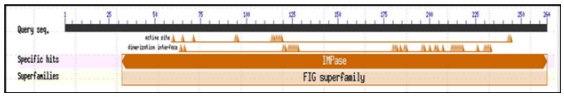

Figure 10. Conserved domain of IMPase protein. The domain shows FIG Superfamily.

The Active site Finder analysis shows a binding cavity which possess the following residues: 70, 90, 92- 95, 194- 196, 213, 220. The least energy value was selected to identify the specific binding site residues of the IMPase protein that interact with its natural receptor FBPase. The binding modes in the protein – receptor complex were analyzed using Discovery Studio Visualizer 3.5. The protein- small ligand binding interactions in the docked complex are presented in Figure 11.

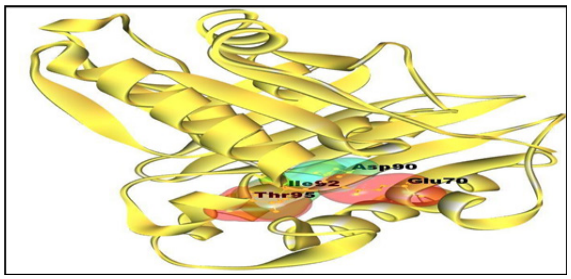

Figure 11. Interaction showing Protein- Small ligand Docking.

Table 4. Active site residues.

RESIDUES	INTERNUCLEAR DISTANCE
GLU 70	2.50 A°
ASP 90	2.38 A° & 2.95 A°
ILE 92	2.49 A°
THR 95	2.85 A°

The table 4 show the binding interactions of the target protein with its natural substrate (FBPse) are GLU 70, ASP 90, ILE 92, THR 95. The above residues participate in binding to FBPase protein.

Conclusion

The homology modeling method provided a reliable structure of IMPase for further investigation. The 3D structure of the IMPase protein generated using 1IMA as a template is comparable to the X-ray resolved protein structure with 93.5% in favorable region in Ramachandran plot, an average 3D-1D score of 84.50

% of the residues is greater than 0.2 (Verify 3D), Z- Score of –5.42 comparable to X – Ray resolved structure (ProSA Server) and 96.17% score in ERRAT infers a reliable model for further research. The secondary structure analysis reveals the 9 Helices, 17 loops, 14 β sheets. Protein-ligand docking of IMPase with its natural receptor confirmed the binding residues in the active site region. The docking studies conclude that GLU 70, ASP 90, ILE 92, THR 95 of IMPase are involved in the binding of protein to receptor signals. Thus, by blocking these residue binding sites, protein regulates glucose metabolism thereby diabetes can be controlled.

Acknowledgements

The author GL and NNT is thankful to The Head, Department of Chemistry and the Principal, University College of Science, Saifabad, Osmania University, Hyderabad and DST FIST, New Delhi for the facilities to carry out this work.

Author Declarations

Funding

No financial support from any agency.

Conflict of Interest

The corresponding author states that there is no conflict of interest.

Ethics approval/declarations (include appropriate approvals or waivers)

Not Applicable.

Availability of Data and material / Data availability

All data generated or analyzed during this study are included in this published article (and its supplementary information files).

Consent to participate

Not applicable

Code availability (software application or custom code) -

Not applicable.

References

1. Diabetes mellitus, fasting blood glucose concentration, and risk of vascular disease: a collaborative meta-analysis of 102 prospective studies. Emerging Risk Factors Collaboration. Sarwar N, Gao P, Seshasai SR, Gobin R, Kaptoge S, Di Angelantonio et al. Lancet. 2010; 26; 375:2215-2222.

2. Causes of blindness and vision impairment in 2020 and trends over 30 years, and prevalence of avoidable blindness in relation to VISION 2020: the Right to Sight: an analysis for the Global Burden of Disease Study GBD 2019 Blindness and Vision Impairment Collaborators* on behalf of the Vision Loss Expert Group of the Global Burden of Disease Study† Lancet Global Health 2021;9: e141-e160.

3. Ying Yang, Yi- Fan Xie, Tai- Mei Zhang, Ling Deng, Li Liao, Shu-Yuan Hu, Yin-Ling Zhang, Fang- Lin Zhang, Da- Qiang. Inositol monophosphatase 1 (IMPA1) promotes triple- negative breast cancer progression through regulating mTOR pathway and EMT process. Cancer Med. 2023; 12:1602-1615. doi: 10.1002/cam4.4970

4. Andreassi C, Luisier R, Crerar H, et al. Cytoplasmic cleavage of IMPA1 3' UTR is necessary for maintaining axon integrity. Cell Rep. 2021;34(8):108778.

5. 9. Pillai RA, Islam MO, Selvam P, et al. Placental Inositol Reduced in Gestational Diabetes as Glucose Alters Inositol Transporters and IMPA1 Enzyme Expression. J Clin Endocrinol Metab. 2021;106(2):e875- e890.

6. 10. Hakim S, Bertucci MC, Conduit SE, Vuong DL, Mitch-

ell CA. Inositol polyphosphate phosphatases in human disease. Curr Top Microbiol Immunol. 2012; 362:247- 314.

7. Garat CV, Crossno JT Jr, Sullivan TM, Reusch JE, Klemm DJ. Inhibition of phosphatidylinositol 3-kinase/Akt signaling attenuates hypoxia-induced pulmonary artery remodeling and suppresses CREB depletion in arterial smooth muscle cells. J Cardiovasc Pharmacol 62: 539 – 548, 2013. doi:10.1097/FJC.0000000000000014.

8. Tang H, Chen J, Fraidenburg DR, Song S, Sysol JR, Drennan AR, Offermanns S, Ye RD, Bonini MG, Minshall RD, Garcia JG, Machado RF, Makino A, Yuan JX. Deficiency of Akt1, but not Akt2, attenuates the development of pulmonary hypertension. Am J Physiol Lung Cell Mol Physiol 308: L208–L220, 2015. doi:10.1152/ajplung.00242.2014.

9. Gardell AM, Yang J, Sacchi R, Fangue NA, Hammock BD, Kültz D. Tilapia (Oreochromis mossambicus) brain cells respond to hyperosmotic challenge by inducing myo-inositol biosynthesis. J Exp Biol 216: 4615– 4625, 2013. doi:10.1242/jeb.088906.

10. Figueiredo T, Melo US, Pessoa AL, Nobrega PR, Kitajima JP, Rusch H, Vaz F, Lucato LT, Zatz M, Kok F, Santos S. A homozygous loss-of-function mutation in inositol monophosphatase 1 (IMPA1) causes severe intellectual disability. Mol Psychiatry 21: 1125–1129, 2016. doi: 10.1038/mp.2015.150.

11. Bone R, Frank L, Springer JP, Pollack SJ, Osborne SA, Atack JR, Knowles MR, McAllister G, Ragan CI, Broughton HB, et al. Structural analysis of inositol monophosphatase complexes with substrates. Biochemistry. 1994 Aug 16;33(32):9460-7. doi: 10.1021/bi00198a011. PMID: 8068620.

12. Chothia, C.; Lesk, A. M. The Relation between the Divergence of Sequence and Structure in Proteins. EMBO J. 1986, 5 (4). https://doi.org/10.1002/j.1460-2075.1986.tb04288.x.

13. Martí-Renom, M. A.; Stuart, A. C.; Fiser, A.; Sánchez, R.; Melo, F.; Šali, A. Comparative Protein Structure Modeling of Genes and Genomes. Annu. Rev. Biophys. Biomol. Struct. 2000, 29 (1). https://doi.org/10.1146/annurev.biophys.29.1.291.

14. Altschul S. Gapped BLAST and PSI-BLAST: A New Generation of Protein Database Search Programs. Nucleic Acids Res. 1997. V. 25. No. 17. P. 3389–3402. doi: 10.1093/nar/25.17.3389

15. Altschul S. Gapped BLAST and PSI-BLAST: A New Generation of Protein Database Search Programs. Nucleic Acids Res. 1997. V. 25. No. 17. P. 3389–3402. doi: 10.1093/nar/25.17.3389

16. A protein secondary structure prediction server. Alexey Drozdetskiy Christian Cole James Procter Geoffrey J. Barton. Nucleic acids research (2015) 43: W1, w389-w394.

17. Improving the sensitivity of progressive multiple sequence alignment through sequence weighting, position specific gap penalties and weight matrix choice. Nucleic Acids res, Thompson JD, Gibson TJ, CLUSTAL W, (1994), 22:4673- 4680.

18. Guex, N.; Peitsch, M. C. SWISS-MODEL and the Swiss-Pdb Viewer: An Environment for Comparative Protein Modeling. Electrophoresis 1997, 18 (15). https://doi.org/10.1002/elps.1150181505.

19. Guex N., Peitsch M.C. SWISS-MODEL and the Swiss-Pdb Viewer: An Environment for Comparative Protein Modeling. Electrophoresis. 1997. V. 18. No. 15. P. 2714–2723. doi: 10.1002/elps.1150181505

20. PROCHECK: a program to check the stereo chemical quality of protein structure. Laskowsky RA, MacArthur MW, Moss DS, Thornton JM (1993), J Appl Crystallography 26: 283- 291.

21. Stereochemical quality of protein structure coordinates. Morris AL, MacArthur Mw, Hutchinson EG, Thornton JM, Proteins (1992), 12:345-364.

22. Stereochemistry of polypeptide chain configurations. Ramachandran GN, Ramakrishnan C, Sasisekharan V, J Mol Biol, (1963), 7:95-99.

23. Half a century of Ramachandran plots, Oliviero Carugo , Kristina Djinovic-Carugo, Acta Crystallographic Section D,2013, 69(8) : 1333-1341.

24. ProSA- web: interactive web service for the recognition of errors in the three – dimensional structure of proteins. Wiederstein M, Sippl MJ, Nucleic Acids res (2007), 35: w407- w410.

25. Laurie AT, J. R. Methods for the Prediction of Protein-Ligand Binding Sites for Structure-Based Drug Design and Virtual Ligand Screening. Curr Protein Pept Sci 2006, 7, 395–406. https://doi.org/10.2174/138920306778559386.

26. Dundas, J.; Ouyang, Z.; Tseng, J.; Binkowski, A.; Turpaz, Y.; Liang, J. CASTp: Computed Atlas of Surface Topography of Proteins with Structural and Topographical Mapping of Functionally Annotated Residues. Nucleic Acids Res. 2006, 34 (Web Server). https://doi.org/10.1093/nar/gkl282.

27. Navaneetha Nambigari*. 2023 Cancer therapeutics: A Structure-based drug design of inhibitors for a novel angiogenic growth factor. Math. Biol. Bioinform. 18(1): 72-88. http://doi.org/10.17537/2023.18.72 (IF = 0.687)

28. Jyothi Bandi, Vasavi Malkhed*and Navaneetha Nambigari*. 2022. An Insilico study of KLK - 14 protein and its inhibition with Curcumin and its derivatives. Chemical Papers. 76, 4955–496. http://doi.org/10.1007/s11696-022-02209-w (IF- 2.097).

29. Navaneetha Nambigari, Kiran Kumar Mustyala, Vasavi Malkhed, Bhargavi Kondagari, Sarita Rajender Potlapally, Ramasree Dulapalli, & Uma Vurupturi*. Angiogenesis: an insilico approach to angiogenic phenotype. Journal of Pharmacy Research. 5 (1): 583 - 588 (2012).

30. Recognition of errors in three-dimensional structures of proteins. Dr. Manfred J. Sippl. December 1993.Proteins 17, 355-362.

31. Lüthy, R., Bowie, J. & Eisenberg, D. Assessment of protein models with three-dimensional profiles. Nature 356, 83–85 (1992). https://doi.org/10.1038/356083a0

32. Colovos C, Yeates TO. Verification of protein structures: patterns of nonbonded atomic interactions. Protein Sci. 1993 Sep;2(9):1511-9. doi: 10.1002/pro.5560020916. PMID: 8401235; PMCID: PMC2142462.